

# JAAS

Accepted Manuscript



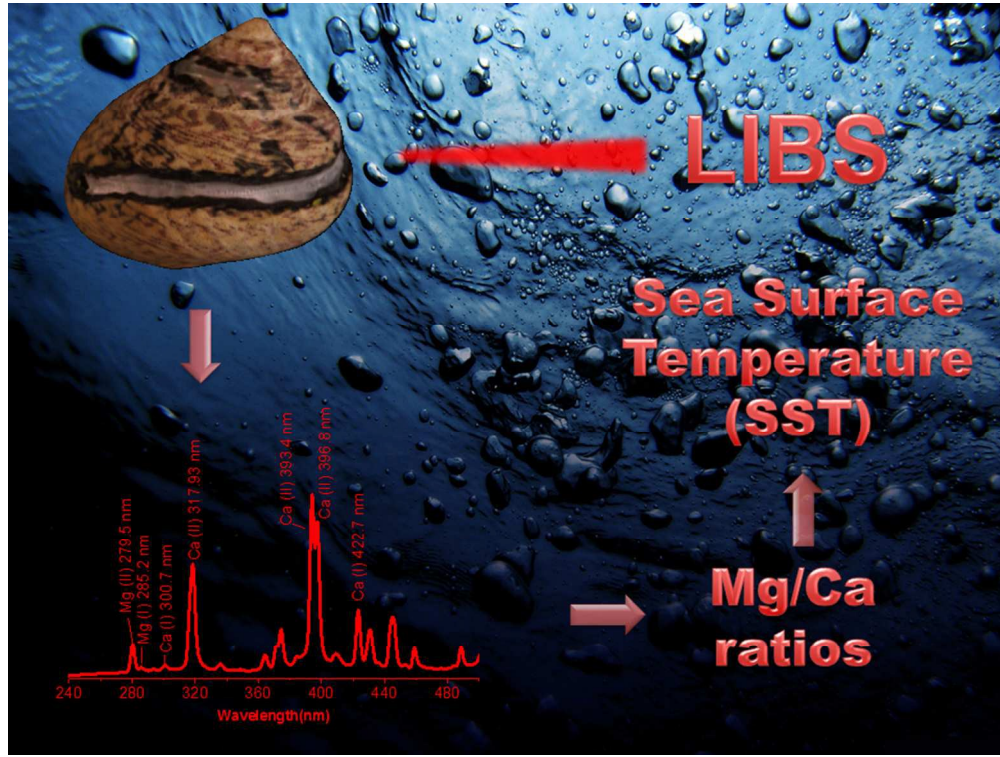
This is an *Accepted Manuscript*, which has been through the Royal Society of Chemistry peer review process and has been accepted for publication.

*Accepted Manuscripts* are published online shortly after acceptance, before technical editing, formatting and proof reading. Using this free service, authors can make their results available to the community, in citable form, before we publish the edited article. We will replace this *Accepted Manuscript* with the edited and formatted *Advance Article* as soon as it is available.

You can find more information about *Accepted Manuscripts* in the [Information for Authors](#).

Please note that technical editing may introduce minor changes to the text and/or graphics, which may alter content. The journal's standard [Terms & Conditions](#) and the [Ethical guidelines](#) still apply. In no event shall the Royal Society of Chemistry be held responsible for any errors or omissions in this *Accepted Manuscript* or any consequences arising from the use of any information it contains.

1  
2  
3  
4  
5  
6  
7  
8  
9  
10  
11  
12  
13  
14  
15  
16  
17  
18  
19  
20  
21  
22  
23  
24  
25  
26  
27  
28  
29  
30  
31  
32  
33  
34  
35  
36  
37  
38  
39  
40  
41  
42  
43  
44  
45  
46  
47  
48  
49  
50  
51  
52  
53  
54  
55  
56  
57  
58  
59  
60



## Mg/Ca ratios measured by Laser Induced Breakdown Spectroscopy (LIBS): a new approach to decipher environmental conditions

A. García-Escárzaga<sup>b§</sup>, S. Moncayo<sup>a§</sup>, Igor Gutiérrez-Zugasti<sup>b§</sup>, M.R. González-Morales<sup>b</sup>, J. Martín-Chivelet<sup>c</sup>, J.O. Cáceres<sup>a\*</sup>

The potential application of Mg/Ca ratios in top shells of the mollusc species *Phorcus lineatus* (Da Costa, 1778) obtained by Laser Induced Breakdown Spectroscopy (LIBS) has been evaluated as an environmental proxy to reconstruct paleotemperatures and season of capture of molluscs for the first time. All samples were collected from Cantabrian Sea (Spain). The results were compared with instrumental sea surface temperatures (SST) and with a known reliable proxy as oxygen isotope ratio ( $\delta^{18}\text{O}_{\text{shell}}$ ) which is mainly dependent on SST, obtained from the same shells. The measurements were taken in two different biominerals of the shell (aragonite and calcite) resulting in a correlation between Mg/Ca ratios and SST of  $R^2 = 0.43$  and  $0.44$ , respectively. Mg/Ca ratios were also studied through a long sequence on three shells collected in autumn 2012. Results show variations in Mg/Ca ratios related to seasonal changes in SST through the year and a good correlation between Mg/Ca ratios and  $\delta^{18}\text{O}_{\text{shell}}$  in two shells ( $R^2 = 0.70$  and  $0.65$ , respectively).

### 1. Introduction

The reconstruction of the climatic and environmental variability in the past lays on the fundamental task of obtaining high-resolution climate and environmental proxies.

<sup>a</sup>Department of Analytical Chemistry, Faculty of Chemistry, Complutense University 28040 Madrid, Spain. Email: jcaceres@ucm.es

<sup>b</sup>Prehistoric International Research Institute of Cantabria, University of Cantabria 39005 Santander Spain.

<sup>c</sup>Department of Stratigraphy, Faculty of Geological Sciences, Complutense University and IGEO Geosciences Institute (CSIC-UCM), 28040 Madrid, Spain.

§ These authors have contributed in equal form

As many of these proxies are based on geochemical parameters, this task requires application of efficient analytical techniques to obtain adequate geological, paleontological, or archaeological record<sup>1</sup>. Biological remains from archaeological sites can provide not only valuable data for reconstructing past climate but can also yield key information about human activities. Among these, mollusc remains are found in many archaeological sites, commonly as

large accumulations of shells as a result of human activity<sup>2</sup>. These shells can be excellent archives of the environmental conditions that existed during the life of the organism (and changes through it, for example, due to seasonal patterns) as well as indicators of human behaviour (e.g., season of capture of molluscs, subsistence strategies, etc<sup>3</sup>)

Most advances in the paleoclimatological analysis of these shells are related to the study of stable isotope ratios, mainly  $\delta^{18}\text{O}$ , which provide information about sea water temperature<sup>4-8</sup>, and much less attention has been paid to other geochemical data of high potential, such as the trace element ratios in the biogenic carbonate. This potential, which is determined by the influence of temperature on the incorporation of chemical elements to the calcium carbonate during shell growth axis is however masked by the difficulties in retrieving significant and accurate data from the shells (for example, from micrometric growth layers) and in interpreting the data, as trace element concentrations are also non-environmental factors dependent.

With the aim of progressing in this direction, this paper presents the study of Mg/Ca ratios in the shells of modern specimens of the mollusc *Phorcus lineatus*, a gastropod abundant in present-day coastal areas and in archaeological sites. The relationship between the Mg/Ca of shell carbonate and the temperature of water has been previously explored for several mollusc species in both laboratory and natural conditions, with remarkably different results. A strong correlation of Mg/Ca with temperature has been shown in experimental work on *Patella rustica* and *Patella caerulea*<sup>9</sup>, *Pecten maximus*<sup>10</sup> and *Pinna nobilis*<sup>11</sup>. However, the correlation is much weaker in the case of *Tridacna gigas*<sup>12</sup>, *Concholetpas concholepas*<sup>13</sup>, *Protothaca staminea*<sup>14</sup>, *Cassostrea virginica*<sup>15</sup> or almost none in *Mesodesma donacium*<sup>16</sup>, *Chione subrugosa*<sup>16</sup>, *Mytilus californianus*<sup>17</sup>, *Artica Islandica*<sup>18,19-20</sup> *Protothaca thaca*<sup>21</sup>.

This paper evaluates, for the first time, the usage of Laser Induced Breakdown Spectroscopy (LIBS)<sup>22,23</sup>, to obtain the Mg/Ca ratios in the shells of modern specimens of the mollusc *Phorcus lineatus*. This

technique provides significant advantages over conventional methods: minimal or no sample preparation, analysis at atmospheric pressure, higher spatial resolution ( $\mu\text{m}$  range), minimally destructive analysis, and good sensitivity<sup>24,25</sup>. Previous works used other analytical techniques such as inductively coupled plasma-atomic emission spectroscopy (ICP-AES)<sup>10,11,26-28</sup>, ICP-mass spectroscopy (ICP-MS)<sup>9,11,21</sup> and laser ablation-ICP-MS<sup>12-14,16,18-21</sup>. These elemental techniques offer high sensitivity and low detection limits. However, all these techniques except the LA-ICP-MS involve wet chemistry processes (dissolution of the sample) that require long sample preparation procedures and microgram order of sample. LA-ICP-MS technique require small sample for its inspection due to reduced size of the sample chamber, moreover the analytical cost is substantially more expensive than LIBS.

In this work, in order to evaluate the potential of Mg/Ca data in the shells of *Phorcus lineatus* to infer sea-water paleotemperatures, a double approach has been accomplished. Firstly, we analysed the Mg/Ca ratio of the shell aperture of different specimens collected monthly in Langre beach (N Spain) through a complete year, in order to know the compositional changes through time and its possible correlation with the sea surface temperature. Secondly, we analysed the variations in Mg/Ca through growth transects in three single shells ("sequential analysis") with the aim of recognizing possible cyclic patterns in compositional data that could correspond with seasonal changes in the temperature.

In a previous study, the samples used in this work were analysed for oxygen stable isotopes for evaluating the usage of the  $\delta^{18}\text{O}_{\text{shell}}$  as a paleothermometer<sup>8</sup>. That study showed that the aragonite of the *P. lineatus* grows under conditions of (or very close to) isotopic equilibrium for the oxygen and that water temperature can thus be inferred from the  $\delta^{18}\text{O}_{\text{shell}}$  if the oxygen isotopic composition of the water is known or can be estimated. These results are incorporated in this paper for comparison and calibration with the Mg/Ca data.

## 2. Material and Methods

### 2.1 Samples

Modern specimens of *P. lineatus* were collected periodically from October 2011 to October 2012 at Langre beach (Fig. 1) in the province of Cantabria-Spain. This mollusc lives up to 10 years and its top shell reaches 35 mm in length with an annual growth rate range of 15 to 26 mm (measured along the centre of the whorl)<sup>29,30</sup>, which allows analysing them along the growth axis covering at least one year. A total of 47 shells were analysed. Table 1 gives the date of collection, SST provided by the Oceanographic Centre of Santander and the samples ID.

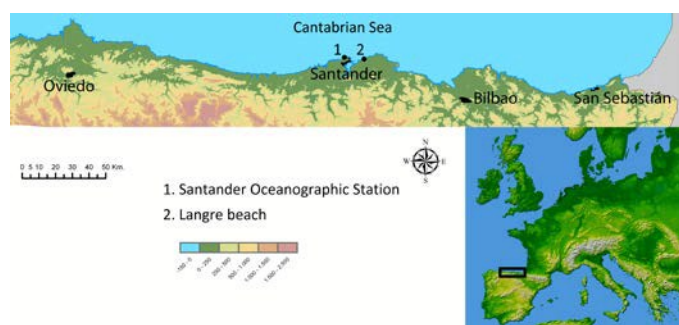


**Fig. 1.** Map of Spanish Cantabrian Coast with the location of the Langre beach and Santander Oceanographic Station.

For cleaning the samples, all the shells were submerged in H<sub>2</sub>O<sub>2</sub> (30%) and H<sub>2</sub>O deionized (70%) solution for 48 hours, they were dried at ambient temperature, then cleaned in an ultrasonic bath for five minutes and finally dried at ambient temperature again.

The microstructure of *P. lineatus* has been studied in previous works using scanning electron microscopy (SEM) and X-ray diffraction (XRD)<sup>31</sup>, showing that they have an outer calcite layer and an inner aragonite layer. The Fig. 2 A&B show the morphology of *P. lineatus* and petrographic microscope images of a top shell microstructure: periostracum coating, prismatic and foliated calcite and aragonite.

Table 1: Top shells collection and SST data.

Sample ID	Collection Date	Mean SST (°C) on the five days prior to shell collection
LANO-07	15/10/2011	17.9
LANO-08	15/10/2011	17.9
LANO-09	12/12/2011	16.6
LANO-10	12/12/2011	16.6
LANO-11	12/12/2011	16.6
LANO-12	25/11/2011	16.1
LANO-13	25/11/2011	16.1
LANO-14	25/11/2011	16.1
LANO-15	24/12/2011	13.6
LANO-16	24/12/2011	13.6
LANO-17	24/12/2011	13.6
LANO-18	12/01/2012	13.6
LANO-19	12/01/2012	13.6
LANO-20	12/01/2012	13.6
LANO-21	10/02/2012	11.8
LANO-22	10/02/2012	11.8
LANO-23	10/02/2012	11.8
LANO-24	23/02/2012	11.7
LANO-25	23/02/2012	11.7
LANO-26	23/02/2012	11.7
LANO-27	25/03/2012	12.8
LANO-28	25/03/2012	12.8
LANO-29	25/03/2012	12.8
LANO-30	22/04/2012	13.0
LANO-31	22/04/2012	13.0
LANO-32	22/04/2012	13.0
LANO-33	05/05/2012	13.8
LANO-34	05/05/2012	13.8
LANO-35	05/05/2012	13.8
LANO-36	03/06/2012	15.3
LANO-37	03/06/2012	15.3
LANO-38	03/06/2012	15.3
LANO-39	21/06/2012	17.5
LANO-40	21/06/2012	17.5
LANO-41	21/06/2012	17.5
LANO-42	22/07/2012	19.4
LANO-43	22/07/2012	19.4
LANO-44	22/07/2012	19.4
LANO-45	05/08/2012	21.0
LANO-46	05/08/2012	21.0
LANO-47	05/08/2012	21.0
LANO-48	02/09/2012	21.5
LANO-49	02/09/2012	21.5
LANO-50	02/09/2012	21.5
LANO-04	01/10/2012	19.1
LANO-05	01/10/2012	19.1
LANO-52	01/10/2012	19.1

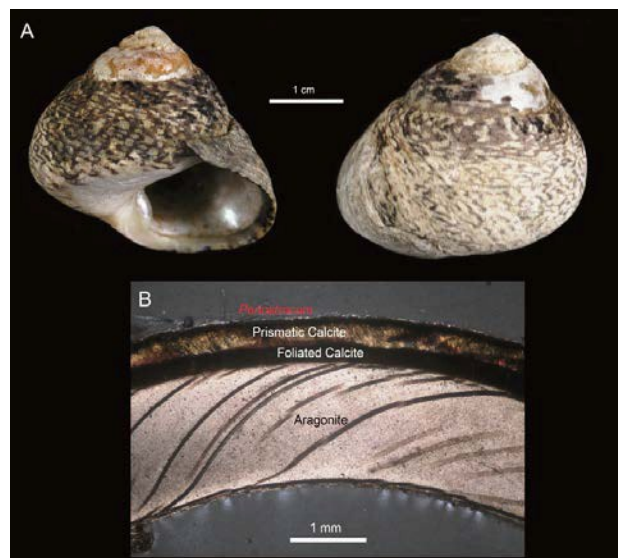


**Fig. 2.** *P. lineatus* specimens: a) Morphology of *P. lineatus* top shell. b) Cross-section showing different crystalline structures: aragonite, foliated and prismatic calcite and the organic periostracum coating.

## 2.2 LIBS set-up

The LIBS technique and the methodology used in the present work together with the most significant experimental conditions have been previously described<sup>32</sup>. Briefly, experiments were performed by using a Q-switched Nd:YAG laser (Quantel, Brio model) operating at 1064 nm, with a pulse duration of 4 ns full width at half maximum. The samples were placed directly over an X–Y–Z manual micrometric positionator with a 0.5  $\mu\text{m}$  step to ensure that each laser pulse impinged on a fresh position. The laser beam was focused onto the sample surface with a 100 mm focal-distance lens, producing a spot of 100  $\mu\text{m}$  in diameter. The laser fluence was fixed to 20 J/cm<sup>2</sup> and the repetition rate was 1 Hz. Emission from the plasma was collected with a 4-mm aperture, with a 7 mm focus fused silica collimator placed at a distance of 3 cm from the sample, and then focused into an optical fiber (with a 1000  $\mu\text{m}$  core diameter and 0.22 numerical aperture), which was coupled to the entrance of the spectrometer. The spectrometer system was a user-configured miniature single-fiber system (EPP2000, StellarNet, Tampa, FL, U.S.A.) with a gated CCD detector. A grating of 300 l/mm

was selected; a spectral resolution of 0.5 nm was achieved with a 7  $\mu\text{m}$  entrance slit. The spectral range used was from 200 to 1000 nm. The detector integration time was set to 1 ms. In order to prevent the detection of bremsstrahlung, the detector was triggered with a 5  $\mu\text{s}$  delay time between the laser pulse and the acquired plasma radiation using a digital delay generator (Stanford model DG535).

## 2.3 LIBS Analysis

For shell analysis, a Dremel microdrill model with a 2 mm drill bit was used for removing the outer layers (i.e. periostracum and calcite layer) when necessary. For LIBS analysis, Mg/Ca ratios were measured in two different biogenic carbonates present in this mollusc: prismatic calcite and aragonite.

Each LIBS spectrum was obtained by averaging 20 laser pulses at the same position. A relative standard deviation (RSD) less than 5% was achieved. The sampling positions were separated by 200  $\mu\text{m}$  covering at least 3.2 cm of shell growth taking approximately 160 LIBS spectra for each sample. The emission lines used for Mg (II) and Ca (I) were 279.55 nm and 422.67 nm, respectively because of their high signal to noise ratio and to avoid the saturation or even the interferences with other emission lines. Fig. 3 shows the crater trace formed by sequential laser shots in both calcite (A) and aragonite (B) layers along the growth of the shells.

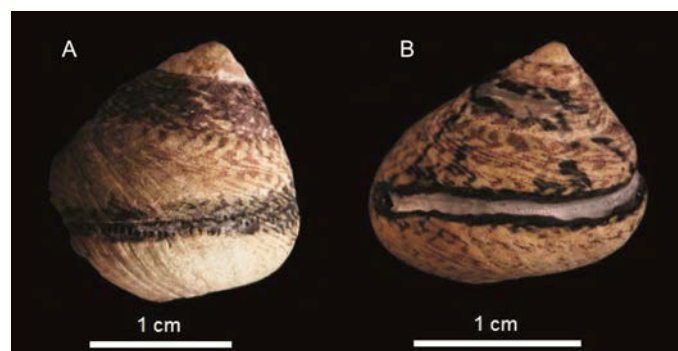


**Fig. 3.** Craters trace formed by laser shots in a) calcite and b) aragonite layers.

### 3. Results and discussion

LIBS experiments were performed on 47 modern shells of *P. lineatus*. Fig. 4 shows typical LIBS spectrum of aragonite layer of the shell covering the range from 240.0 nm to 500.0 nm. The assignment of the emission lines from main elements at their corresponding wavelengths was done based on the NIST atomic spectra database<sup>33</sup>. The most representative lines in nm were Mg I (285.2), Mg II (279.5), Ca I (300.7; 422.7) and Ca II (317.9; 393.4; 396.8). Due to the morphology of the sample (spiral) in order to keep the same focusing condition, each measurement along the mollusc growth was corrected by means of a x-y-z micrometric-positioner avoiding the defocusing effect and enhancing the reproducibility of the measurements.

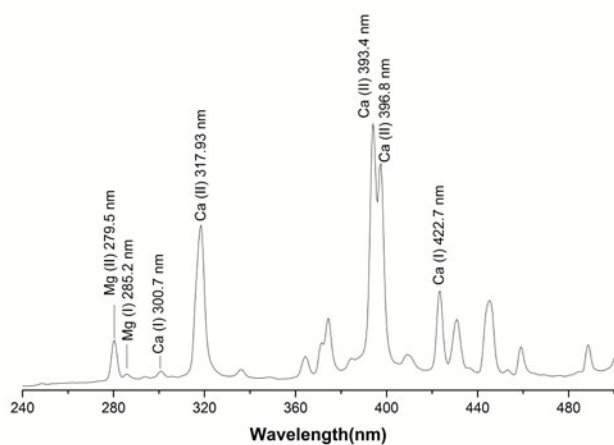


Fig. 4. LIBS spectrum of *P. lineatus* sample

#### 3.1. Mg/Ca ratios from shell aperture samples

The annual correlation between SST and the Mg/Ca ratios in aragonite and calcite layers obtained for 47 *P. lineatus* top shells are shown in Fig. 5A & B. Each value of the Mg/Ca ratio was obtained by averaging the first four values of the shell aperture for three different shells collected on the same day. The error bars represent the relative standard deviation (RSD) between shell specimens. The highest Mg/Ca ratio was found in the calcite layer, 0.319, whereas in the aragonite layer it was 0.06. This difference is attributed to the fact that calcite and magnesium

carbonate have hexagonal crystalline structure, and therefore solid solutions between these two phases occur frequently<sup>34</sup>. Moreover, the atomic radius of Ca and Mg are similar and Mg could be easily incorporated into the calcite structure. On the other hand, the aragonite layer has an orthorhombic crystalline structure, making the incorporation of Mg unfavourable<sup>35, 36</sup>. The relation between Mg/Ca ratios and SST is inverse (Fig. 5A) in aragonite layer whereas directly proportional in calcite layer (Fig. 5B). Therefore, an increase in the Mg/Ca ratios measured in the calcite is observed in periods of high temperature, while measurements in the aragonite showed increased elemental ratios during colder conditions. A correlation coefficient ( $R^2$ ) of 0.43 and 0.44 was obtained between Mg/Ca ratios for aragonite and calcite layers with SST, respectively. This correlation in the Mg/Ca ratios demonstrates that incorporation of magnesium in biogenic carbonates is not only influenced by temperature changes but also by other factors such as salinity, food quality and quantity and reproductive cycles, among others<sup>37</sup>. Nevertheless, the concentration of an element in a specific position on the growth axis is substantially homogeneous within a layer and thus no significant variations in the elemental ratios are observed with the depth of the crater. Furthermore, the high RSD values of 30.7% and 25.9% in aragonite and calcite respectively for different shells collected on the same day, reflect the variability between specimens of the same species growing in the same environmental conditions, which indicates that the incorporation of trace elements is physiologically controlled by factors such as metabolism, kinetic effects, calcification rates, differences in crystal growth orientation and the morphology.<sup>11,26,27,38,39</sup>

#### 3.2. Mg/Ca ratios from sequential samples

Three top shells were analysed by LIBS along their growth axes considering at least one year. Mg/Ca ratios from LANO-4 and LANO-5 shells were measured only on the aragonite layer, whereas LANO-52 was measured in both aragonite and prismatic calcite layers.

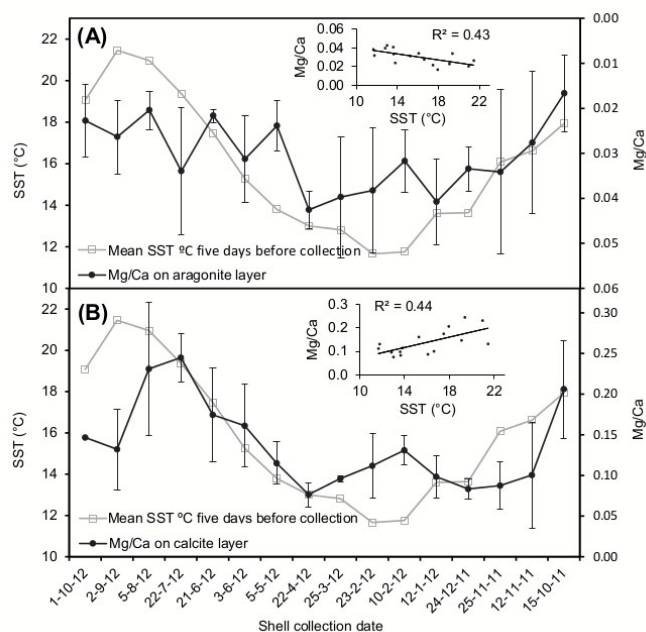


**Fig. 5.** Annual correlation between SST and Mg/Ca Ratio in a) aragonite layer and b) calcite.

The sequence obtained from LANO-4, LANO-5 and LANO-52 aragonite samples (Fig. 6A, B & C) shows minimum values in the first 13-15 mm from the shell aperture, increasing quickly in the next 10-12 mm, and decreasing again. Similar trend was observed for all specimens collected on the same day. This sinusoidal pattern is related to seasonal changes in SST through the year, with maximum values exhibiting lower temperatures. The sequence of LANO-52 from the prismatic calcite layer (Fig. 6D) had an inverse behaviour, with Mg/Ca increasing during warmer months and decreasing in winter. The results obtained in calcite and aragonite are in accordance with the expected trends and with results from shell aperture samples. The incorporation of Mg as an impurity in calcite is endothermic<sup>40</sup>, therefore more amount of this element is incorporated into the crystal at higher temperatures, as opposed to aragonite layer.

Finally, isotope sequences from LANO-5 and LANO-52 in the aragonite layer were compared with Mg/Ca ratios<sup>8</sup>. Mean of four LIBS measurements of

elemental ratios corresponded approximately to one isotope measurement.

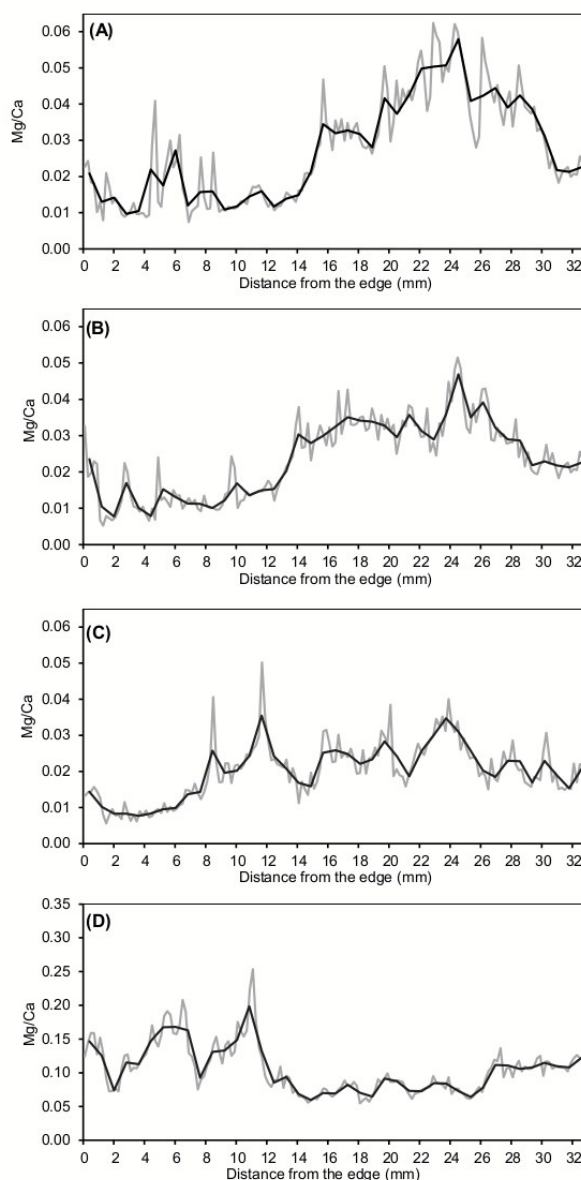


**Fig. 6.** Mg/Ca ratios along the growth direction in four top shells, the first two A) LANO-4, B) LANO-5 were measured in the aragonite layer and last one LANO-52 in both C) aragonite and D) calcite layer. Grey lines show result obtained on each point measured and black lines show the average of four Mg/Ca values.

A high correlation value between Mg/Ca ratios and  $\delta^{18}\text{O}_{\text{shell}}$  was found ( $R^2 = 0.7$ ) in the case of LANO-5 (Fig. 7A), but not in the case of LANO-52, that



presents a low correlation ( $R^2=0.07$ ). Nonetheless, if we use only the last 16 mm of growth of LANO-52 (Fig. 7B), the correlation becomes significant ( $R^2=0.65$ ). This anomaly, observed in the portions of growth after 16 mm in LANO-52, is difficult to explain, although could be mentioned that the elemental ratios are not only dependent of SST.

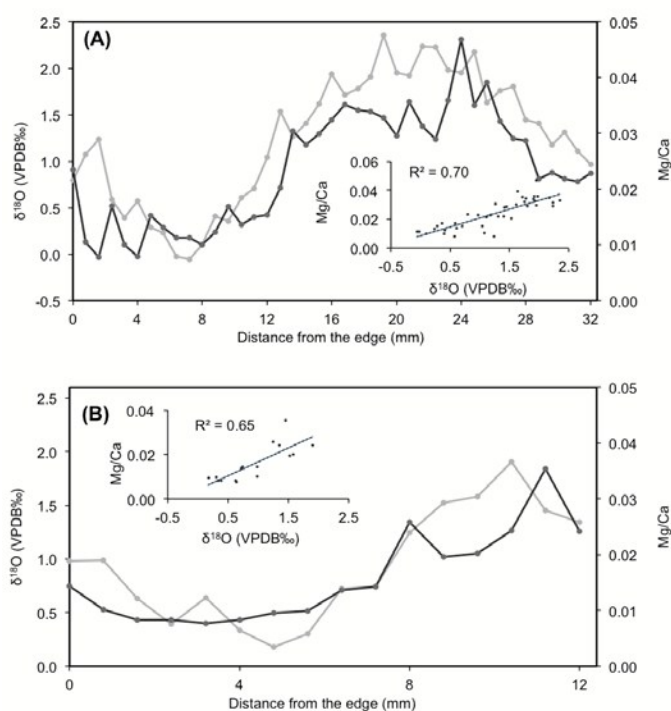


**Fig. 7.** Relation between  $\delta^{18}\text{O}_{\text{shell}}$  and Mg/Ca ratios in *P. lineatus* top shells along the growth axes. A) LANO-5 B) LANO-52.

If we considered the correlation obtained from LANO-5 and the first middle part of LANO-52, the correlations presented in this paper is among the highest determination coefficients documented until date, since only Ferguson et al<sup>9</sup> and Freitas et al<sup>10</sup> published a higher correlation on limpets ( $R^2=0.79$ ) and scallops ( $R^2=0.77$ ), respectively

#### 4. Conclusions

The use of Mg/Ca ratios obtained by LIBS technique in mollusc species as paleoclimatic proxy has been reported for the first time. The analyses of Mg/Ca ratios on *P. lineatus* using LIBS technique provides

successful results, showing the great potential of the technique for environmental analysis and as marker of seasonality. Tracing past environmental conditions is crucial for many disciplines, such as palaeoclimatology, archaeology, palaeoceanography or palaeontology, and establishing the season of capture has important implications particularly for archaeological studies, since it is a key issue for the reconstruction of settlement patterns and subsistence strategies of hunter-fisher-gatherers.

The correlation coefficients between Mg/Ca ratios and  $\delta^{18}\text{O}_{\text{shell}}$  suggest that the incorporation of trace elements in the calcium carbonate of *P. lineatus* is not only dependent on the environmental temperature, but also by other factors such as salinity, food quality and quantity, reproductive cycles and others, although the information obtained did not allow to know the causes that are involved in the process of shell formation.

The feasibility of LIBS technique as analytical methodology for the determination of climate patterns and their correlation with other techniques as  $\delta^{18}\text{O}$  and finally with the temperature has pointed out LIBS as an analytical technique appropriate to perform elemental analysis of mollusc shells. In addition, LIBS allows to obtain fast results and considerable cost reduction without loss of archaeological material. However, further work is needed to improve the correlation coefficients and determine the influence of other parameters in the incorporation of Mg to the different allotropic forms of carbonate in the shell molluscs.

#### Acknowledgements

This research was performed as part of the project "The human response to the global climatic change in a littoral zone: the case of the transition to the Holocene in the Cantabrian coast (10,000-5000 cal BC) (HAR2010-22115-C02-01)" funded by the Spanish Ministry of Economy and Competitiveness. Two of the authors AGE and IGZ were supported by a predoctoral grant from the University of Cantabria and a contract of the Juan de la Cierva programme funded by the Spanish Government, respectively. We must thank the Fishing Activity Service of the

Cantabrian Government for the authorization to collect the modern *P. lineatus*, the Aquaculture Facility of Santander's Oceanographic Center for providing the information related to sea surface temperatures, José Ramón Mira Soto for his help measuring salinity and Adolfo Cobo García for his comments. The material and resources were provided by the Instituto Internacional de Investigaciones Prehistóricas de Cantabria (IIIPC), the University of Cantabria and the Complutense University of Madrid.

## References

- 1 I. Burton, B. Challenger, S. Huq, R. J. T. Klein and G. Yohe, *Adaptation to Climate Change in the Context of Sustainable Development and Equity*, Chap 18. IPCC Working Group II Washington DC, USA. 2001.
- 2 M. Álvarez, I. Briz Godino, A. Balbo and M. Madella, *Quat. Int.*, 2011, **239**, 1–7.
- 3 C. F. T. Andrus, *Quat. Sci. Rev.*, 2011, **30**, 2892–2905.
- 4 A. C. Colonese, S. Troelstra, P. Ziveri, F. Martini, D. Lo Vetro and S. Tommasini, *J. Archaeol. Sci.*, 2009, **36**, 1935–1944.
- 5 A. L. Prendergast, M. Azzopardi, T. C. O'Connell, C. Hunt, G. Barker and R. E. Stevens, *Chem. Geol.*, 2013, **345**, 77–86.
- 6 T. Wang, D. Surge and S. Mithen, *Palaeogeogr. Palaeoclimatol. Palaeoecol.*, 2012, **317–318**, 104–113.
- 7 M. A. Mannino, K. D. Thomas, M. J. Leng and H. J. Sloane, *Geo-Mar. Lett.*, 2008, **28**, 309–325.
- 8 I. Gutierrez Zugasti, A. Garcia Escarzaga, J. Martín-Chivelet and M. R. Gonzalez-Morales, *The Holocene*. 2015, **25**, 1002–1014.
- 9 J. E. Ferguson, G. M. Henderson, D. A. Fa, J. C. Finlayson and N. R. Charnley, *Earth Planet. Sci. Lett.*, 2011, **308**, 325–333.
- 10 P. S. Freitas, L. J. Clarke, H. Kennedy and C. A. Richardson, *Chem. Geol.*, 2012, **291**, 286–293.
- 11 P. Freitas, L. J. Clarke, H. Kennedy, C. Richardson and F. Abrantes, *Geochem. Geophys. Geosystems*, 2005, **6**, n/a–n/a.
- 12 M. Elliot, K. Welsh, C. Chilcott, M. McCulloch, J. Chappell and B. Ayling, *Palaeogeogr. Palaeoclimatol. Palaeoecol.*, 2009, **280**, 132–142.
- 13 C. E. Lazareth, N. Guzman, F. Poitrasson, F. Candaudap and L. Ortlieb, *Geochim. Cosmochim. Acta*, 2007, **71**, 5369–5383.
- 14 R. K. Takesue and A. van Geen, *Geochim. Cosmochim. Acta*, 2004, **68**, 3845–3861.
- 15 D. Surge and K. C. Lohmann, *J. Geophys. Res. Biogeosciences*, 2008, **113**, G02001.
- 16 M. Carré, I. Bentaleb, O. Bruguier, E. Ordinola, N. T. Barrett and M. Fontugne, *Geochim. Cosmochim. Acta*, 2006, **70**, 4906–4920.
- 17 H. L. Ford, S. A. Schellenberg, B. J. Becker, D. L. Deutschman, K. A. Dyck and P. L. Koch, *Paleoceanography*, 2010, **25**, PA1203.
- 18 L. C. Foster, A. A. Finch, N. Allison, C. Andersson and L. J. Clarke, *Chem. Geol.*, 2008, **254**, 113–119.
- 19 B. R. Schöne, Z. Zhang, P. Radermacher, J. Thébaud, D. E. Jacob, E. V. Nunn and A.-F. Maurer, *Palaeogeogr. Palaeoclimatol. Palaeoecol.*, 2011, **302**, 52–64.
- 20 H. Toland, B. Perkins, N. Pearce, F. Keenan and M. J. Leng, *J. Anal. At. Spectrom.*, 2000, **15**, 1143–1148.
- 21 C. E. Lazareth, F. Le Cornec, F. Candaudap and R. Freydier, *Palaeogeogr. Palaeoclimatol. Palaeoecol.*, 2013, **373**, 39–49.
- 22 D. A. Cremers and L. J. Radziemski, *Handbook of laser-induced breakdown spectroscopy*, Wiley-Blackwell, Oxford - UK, 2nd Ed., 2013.
- 23 *Laser-Induced Breakdown Spectroscopy - Theory and Applications*, Springer, Milan, Italy, Sergio Musazzi, Umberto Perini., 2014, vol. 182.
- 24 F. J. Fortes, I. Vadillo, H. Stoll, M. Jiménez-Sánchez, A. Moreno and J. J. Laserna, *J. Anal. At. Spectrom.*, 2012, **27**, 868–873.
- 25 A. Marín-Roldán, J. A. Cruz, J. Martín-Chivelet, M. J. Turrero, A. I. Ortega and J. O. Caceres, *J. Appl. Laser Spectrosc.*, 2014, **1**, 7–12.
- 26 P. S. Freitas, L. J. Clarke, H. Kennedy, C. A. Richardson and F. Abrantes, *Geochim. Cosmochim. Acta*, 2006, **70**, 5119–5133.
- 27 P. S. Freitas, L. J. Clarke, H. A. Kennedy and C. A. Richardson, *Biogeosciences*, 2008, **5**, 1245–1258.
- 28 P. S. Freitas, L. J. Clarke, H. Kennedy and C. A. Richardson, *Biogeosciences*, 2009, **6**, 1209–1227.
- 29 J. M. Gaillard, *Aspects qualitatifs et quantitatifs de la croissance de la coquille de quelques espèces de Mollusques Prosobranches en fonction de la latitude et des conditions écologiques*, Mémoires du musée National d'Historie Naturelle. Éditions du Muséum. Lahure- Fr. 1965, 38 1-55.

- 1  
2  
3  
4 30 M. B. Regis, *J. Molluscan Stud.*, 1972, **3**, 259–267.  
5 31 M. A. Mannino, B. F. Spiro and K. D. Thomas, *J.*  
6 *Archaeol. Sci.*, 2003, **30**, 667–679.  
7 32 S. Moncayo, S. Manzoor, T. Ugidos, F. Navarro-  
8 Villoslada and J. O. Caceres, *Spectrochim. Acta Part*  
9 *B At. Spectrosc.*, 2014, **101**, 21–25.  
10 33 NIST Atomic Spectra Database. US Department of  
11 Commerce, [http://physics.nist.gov](http://physics.nist.gov/PhysRefData/ASD/lines_form.html)  
12 [/PhysRefData/ASD/lines\\_form.html](http://physics.nist.gov/PhysRefData/ASD/lines_form.html) (Cited June 5  
13 2015).  
14 34 R. M. Hazen, R.T. Downs, A.P. Jones and L. Kah,  
15 *Rev. Mineral. Geochem.* 2013, **75**, 7–46.  
16 35 A. A. Finch and N. Allison. *Geophys. Res. Lett.* 2008,  
17 **35**, L08704.  
18 36 O.Branson, S.A.T. Redfern, T.Tyliszczak, A.  
19 Sadekov,G.Langer, K.Kimoto, H.Elderfield. *Earth*  
20 *Planet. Sci. Lett.* 2013, **383**, 134–141  
21 37 H. Toland, B. Perkins, N. Pearce, F. Keenan and M. J.  
22 Leng, *J. Anal. At. Spectrom.*, 2000, **15**, 1143–1148.  
23 38 A. Lorrain, D. P. Gillikin, Y.-M. Paulet, L. Chauvaud,  
24 A. L. Mercier, J. Navez and L. André, *Geology*, 2005,  
25 **33**, 965–968.  
26 39 E. V. Putten, F. Dehairs, E. Keppens and W. Baeyens,  
27 *Geochim. Cosmochim. Acta*, 2000, **64**, 997–1011.  
28 40 A. Katz, *Geochim. Cosmochim. Acta*, 1973, **37**, 1563–  
29 1586.  
30  
31  
32  
33  
34  
35  
36  
37  
38  
39  
40  
41  
42  
43  
44  
45  
46  
47  
48  
49  
50  
51  
52  
53  
54  
55  
56  
57  
58